Progress of Theoretical Physics, Vol. 65, No. 6, June 1981

General Relativistic Collapse of Axially Symmetric Stars Leading to the Formation of Rotating Black Holes

Takashi NAKAMURA

Research Institute for Fundamental Physics
Kyoto University, Kyoto 606

(Received November 1, 1980)

Numerical calculations have been made for the formation process of axisymmetric, rotating black holes of $10M_{\odot}$. The initial density of a star is about 3×10^{13} g/cm^3. Numerical results are classified mainly by q which corresponds to $|a|/M$ in a Kerr black hole. For $q\lesssim0.3$, the effect of rotation to the gravitational collapse is only to make the shape of matter oblate. For $0.3\lesssim q\lesssim0.95$, although the distribution of matter is disk-like, a ring-like peak of proper density appears. This ring is inside the apparent horizon, which is always formed in the case $q\lesssim0.95$. For $q\gtrsim0.95$, no apparent horizon is formed. The distribution of matter shows a central disk plus an expanding ring. It is found that electromagnetic-like field in the $[(2+1)+1]$-formalism plays an important role in a formation of a rotating black hole. Local conservation of angular momentum is checked. Accuracy of constraint equations is also shown to see the truncation error in the numerical calculations.

§ 1. Introduction

Stationary solutions to Einstein's vacuum field equations have been studied very well. On the assumption that all singularities in space-time are hidden behind the non-singular event horizon, the Israel-Carter[1),2)] theorem tells us that solutions form discrete continuous families each depending on, at most, two parameters. Robinson[3)] proved that the Kerr family with $|a|<M$ is the unique one of the Israel-Carter theorem. On the other hand if the above assumption is not adopted many other stationary solutions[4)] have been obtained.

In the realistic gravitational collapse a star collapses from the region of slow motion and weak gravity to that of fast motion and strong gravity. The structure of the latter region will depend on the initial conditions. Therefore neither the assumption on this structure nor the special stationary solution but the dynamical process does determine the ultimate fate of the gravitational collapse. For a spherically symmetric case, Yodzis et al.[5)] showed a possibility of the existence of a naked singularity. For a non-spherical case, Nakamura et al.[6)] suggested that a naked singularity may appear in a prolate collapse if the initial quadrupole moment is large enough. These results tell us that naked singularity may appear in the realistic collapse of a star under a certain initial condition.

To know the dynamical process of collapse of a star, it is necessary to inte-

grate the Einstein equations as an initial value problem by using a realistic equation of state. This problem will not be solved analytically because solutions will not be expressed by analytic functions. Only numerical relativity will give us the answer to this problem. In this paper we present numerically generated black holes with rotation. In § 2, the basic equations of the problem are given. In § 3, initial conditions and coordinate conditions are shown. In § 4, results of the numerical calculations are shown. In § 5, some discussions will be made.

§ 2. Basic equations

We adopt a [(2+1)+1]-formalism[7] of the Einstein equations. In this formalism the Einstein equations become

$$\partial_0 H_{AB} = -2\alpha\chi_{AB} + \eta_{A\|B} + \eta_{B\|A}\,, \tag{2·1}$$

$$\begin{aligned}\partial_0\chi_{AB} - \eta^C\chi_{AB\|C} = {}& \alpha[{}^{(2)}R_{AB} + \chi\chi_{AB}] - 2\alpha\chi_A{}^C\chi_{CB} \\ & - \alpha_{\|A\|B} + (\chi_{AC}\eta^C_{\|B} + \chi_{BC}\eta^C_{\|A}) - \alpha\lambda^{-1}\lambda_{\|A\|B} + \alpha K_\phi{}^\psi\chi_{AB} \\ & - \frac{1}{2}\alpha[\varepsilon_{CA}\varepsilon_{DB}E^CE^D - H_{AB}(E_CE^C - B_\phi{}^2)] \\ & - 8\pi\alpha\left[S_{AB} + \frac{1}{2}H_{AB}(\rho_H - S_c{}^c - \lambda^{-2}\mathcal{J})\right],\end{aligned} \tag{2·2}$$

$$\partial_0\lambda - \eta^A\partial_A\lambda = -\alpha\lambda K_\phi{}^\psi\,, \tag{2·3}$$

$$\begin{aligned}\partial_0 K_\phi{}^\psi - \eta^A\partial_A K_\phi{}^\psi = {}& \alpha K_\phi{}^\psi(K_\phi{}^\psi + \chi) - H^{AB}(\partial_A\alpha)(\partial_B\lambda)\lambda^{-1} \\ & - \alpha^{(2)}\Delta\lambda\cdot\lambda^{-1} - \frac{1}{2}\alpha[E_AE^A - B_\phi{}^2] \\ & - 4\pi\alpha(\rho_H - S_A{}^A + \lambda^{-2}\mathcal{J}),\end{aligned} \tag{2·4}$$

$$\chi^2 - \chi^{AB}\chi_{AB} + {}^{(2)}R = 2\lambda^{-1}{}^{(2)}\Delta\lambda - 2\chi K_\phi{}^\psi + \frac{1}{2}(E_AE^A + B_\phi{}^2) + 16\pi\rho_H\,, \tag{2·5}$$

$$\lambda^{-1}(\lambda\chi_A{}^B)_{\|B} - \lambda^{-1}(\partial_A\lambda)K_\phi{}^\psi - \partial_A(\chi + K_\phi{}^\psi) = 8\pi J_A - \frac{1}{2}B_\phi\cdot\varepsilon_{CA}E^C, \tag{2·6}$$

$$\begin{aligned}\partial_0(\lambda^2\sqrt{H}\,E^A) = {}& (\eta^B(\lambda^2E^A)_{\|B} + \varepsilon^{AB}\eta^C_{\|B}\varepsilon_{DC}\lambda^2E^D)\sqrt{H} \\ & + \sqrt{H}\,\varepsilon^{AB}\partial_B(\alpha\lambda^2B_\phi) - 16\pi\alpha\lambda S^A\sqrt{H}\,,\end{aligned} \tag{2·7}$$

$$\partial_0(B_\phi\sqrt{H}\,\lambda^{-1}) = \partial_A(\eta^A\sqrt{H}\,B_\phi\lambda^{-1}) + \partial_A(\alpha E_B\varepsilon^{BA}\sqrt{H}\,\lambda^{-1}) \tag{2·8}$$

and

$$(\lambda^2E^A)_{\|A} = 16\pi\lambda J_\phi\,. \tag{2·9}$$

In Eqs. (2·1) to (2·9), ${}^{(2)}\Delta$, $\|$, ${}^{(2)}R$ and ${}^{(2)}R_{AB}$ are Laplacian, covariant differentiation, scalar curvature and Ricci tensor with respect to H_{AB}, respectively. The derivation of Eqs. (2·1) to (2·9) and the definition of various quantities appeared are shown in the Appendix. Note that Eqs. (2·7) to (2·9) strongly resemble the Maxwell equations. We assume the perfect fluid for $T_{\mu\nu}$,

$$T_{\mu\nu}=\rho(1+\varepsilon+p/\rho)u_\mu u_\nu+pg_{\mu\nu}\,, \tag{2·10}$$

where ρ, ε and p are proper mass density, internal energy per gram and pressure, respectively. According to Maeda et al.,[7] the hydrodynamics equations can be written by using J_A, J_ϕ and ρ_H. In this paper we use different expressions of the hydrodynamics equations from those in Ref. 7).

i) Energy equation

$$\begin{aligned}&\partial_0(\alpha u^0\sqrt{H}\lambda\varepsilon\rho)+\partial_A(\alpha u^0\sqrt{H}\lambda U^A\varepsilon\rho)\\&\quad=-p\,[\partial_0(\alpha u^0\sqrt{H}\lambda)+\partial_A(\alpha u^0\sqrt{H}\lambda U^A)].\end{aligned} \tag{2·11}$$

ii) Euler equations

$$\begin{aligned}&\partial_0(\lambda\sqrt{H}\cdot J_A)+\partial_B(U^B\lambda\sqrt{H}J_A)\\&\quad=-\alpha\lambda\sqrt{H}(\partial_A p+(p+\rho_H)(\partial_A\alpha)\alpha^{-1})\\&\qquad+\alpha\lambda\sqrt{H}(p+\rho_H)\Big[\frac{1}{2}(\partial_A H_{BC})V^BV^C+\alpha^{-1}V_C\partial_A\eta^C\Big]\\&\qquad+\alpha\lambda\sqrt{H}\lambda^{-1}J_\phi[E_A+\varepsilon_{AC}(2B_\phi V^C-\lambda^{-2}\varepsilon^{CB}\partial_B\lambda\cdot V^\phi)].\end{aligned} \tag{2·12}$$

iii) Conservation of angular momentum

$$\partial_0(\lambda\sqrt{H}J_\phi)+\partial_A(U^A\lambda\sqrt{H}J_\phi)=0\,. \tag{2·13}$$

iv) Conservation of baryon number

$$\partial_0(\alpha u^0\sqrt{H}\lambda\rho)+\partial_B(U^B\alpha u^0\sqrt{H}\lambda\rho)=0\,. \tag{2·14}$$

v) Equation of state

$$p=p(\rho,\varepsilon). \tag{2·15}$$

vi) Normalization of four-velocity

$$\alpha u^0=1/\sqrt{1-V^BV_B-V^\phi V_\phi}\,, \tag{2·16}$$

where

$$V^B=(p+\rho_H)^{-1}J^B\,,\qquad V^\phi=(p+\rho_H)^{-1}J_\phi$$

and

$$U^A=\alpha V^A-\eta^A.$$

The basic flow of the numerical calculation is the same as that adopted by Nakamura et al.[8] We adopt cylindrical coordinates R, Z and ϕ. We assume that the system has reflection symmetry about the $Z=0$ plane. In this case the requlrity conditions and the reflection symmetry enable us to use the following basic variables instead of the original variables appeared in Eqs. (2·1) to (2·16):

$$B\equiv\lambda/R\,,\qquad a\equiv(\sqrt{H}_{RR}-B)/R^2\,,\qquad c\equiv H_{RZ}/(RZ),$$
$$F\equiv\sqrt{H}_{ZZ}\,,\qquad k_R{}^R\equiv(\chi_R{}^R-K_\phi{}^\phi)/R^2,\qquad k_R{}^Z\equiv\chi_R{}^Z/(RZ),$$
$$K_Z{}^Z\equiv\chi_Z{}^Z\,,\quad e^R\equiv E^R/R^2,\quad e^z\equiv E^Z/(RZ),\quad b_\phi\equiv B_\phi/(R^2Z),$$
$$\tilde{\eta}^R\equiv\eta^R/R\,,\quad \tilde{\eta}^Z\equiv\eta^Z/Z\,,\quad Q_b\equiv\alpha u^0B\sqrt{H}\rho\,,\quad h=1+\varepsilon+p/\rho\,,$$
$$Q_R\equiv B\sqrt{H}J_R/Q_b/R\,,\qquad Q_z\equiv B\sqrt{H}J_z/Q_b/Z\,,$$
$$\Omega\equiv B\sqrt{H}J_\phi/Q_b/R^2,\qquad \alpha u^0\equiv B\sqrt{H}(\rho_H+p)/h/Q_b\,,$$
$$\tilde{V}^R\equiv V^R/R\,,\quad \tilde{V}^Z\equiv V^Z/Z\,,\quad \tilde{U}^R\equiv\alpha\tilde{V}^R-\tilde{\eta}^R,\quad \tilde{U}^z\equiv\alpha\tilde{V}^z-\tilde{\eta}^Z.\qquad(2\cdot17)$$

By this choice of the basic variables, we do not need to worry about a cusp or a bump of the variables which occurs in Wilson's code[9] because the regularity conditions are automatically satisfied. To write down the basic equations by using our variables is rather tedious but straightforward.

A method of finite difference is the same as that in Ref. 8). We use x and y instead of R and Z where $x=R^2$ and $y=Z^2$. Dynamical equations appeared in Eqs. (2·1) to (2·16) can be written in the form

$$\partial_0Q=2x\partial_x(QW^R)+2y\partial_y(QW^Z)+S\,,$$
$$W^R=\tilde{\eta}^R\text{ or }\tilde{U}^R\quad\text{and}\quad W^Z=\tilde{\eta}^Z\text{ or }\tilde{U}^Z\,,\qquad(2\cdot18)$$

where S is the source term for Q. The finite difference is taken as

$$Q(t+\Delta t,x,y)=Q(t,x,y)+\Delta tS$$
$$+\Delta t[\text{donor cell type finite difference for }\partial_x(QW^R)\text{ and }\partial_y(QW^Z)].$$

For the evolution equations of space-time geometry, Friedrichs-Lax type viscosity terms are added to Eq. (2·18). As we can see later, these viscosity terms are not so large that their effect to the numerical solution is small. For the conservation laws such as Eqs. (2·13) and (2·14), a different finite difference is taken. Equations (2·13) and (2·14) can be written as

$$\frac{\partial Q}{\partial t}+\frac{1}{R}\frac{\partial}{\partial R}R^2\tilde{U}^RQ+\frac{\partial}{\partial Z}Z\cdot\tilde{U}^ZQ=0\,.\qquad(2\cdot19)$$

If either R or Z is zero, for example, if R is zero, Eq. (2·19) can be written as

$$\frac{\partial Q}{\partial t}+2\tilde{U}^R Q+\frac{\partial}{\partial Z}Z\tilde{U}^Z Q=0\,. \tag{2·20}$$

We apply the donor cell type difference only to the third term of Eq. (2·20).

§ 3. Initial conditions and coordinate conditions

i) *Initial conditions*

We use the following initial condition:

$$\rho_H=(2\pi\lambda)^{-3/2}\cdot\exp(-(x+y)/2/\lambda^2)/\phi^6,$$
$$Q^R=Q^Z=0\,,\qquad J_\phi=\rho_H\cdot\Omega_0\cdot\exp(-x/2/\lambda^2)x\,,$$
$$c=a=0\,,\qquad B=F=\phi^2\,,\qquad K_\phi{}^\phi=k_R{}^R=k_R{}^Z=k_Z{}^Z=0\,,$$
$$b_\phi=0\,,\qquad e^R=-4/\phi^2\cdot\partial_x W\quad\text{and}\quad e^Z=-4/\phi^2\cdot\partial_y W\,. \tag{3·1}$$

As this condition is the same as that in Ref. 8), ϕ and W are determined by

$$4(\partial_x\phi+x\partial_{xx}\phi)+2\phi_y+4y\partial_{yy}\phi$$
$$=-2\pi(\rho_H\phi^6)\phi^{-1}-\phi^5 x(x(\partial_x W)^2+y(\partial_y W)^2) \tag{3·2}$$

and

$$(8+24x(\partial_x\phi)\phi^{-1})\partial_x W+4x\partial_{xx}W$$
$$+(2+24y(\partial_y\phi)\phi^{-1})\partial_y W+4y\partial_{yy}W=8\pi J^\phi x^{-1}. \tag{3·3}$$

A method of solving Eqs. (3·2) and (3·3) is given in Ref. 8). As an equation of state, we use

$$p=\begin{cases}1/3\rho\varepsilon & \text{for}\quad \rho\le\rho^*\equiv 3\times10^{14}\mathrm{g/cm^3},\\ (\rho-\rho^*)\varepsilon+1/3\rho^*\varepsilon & \text{for}\quad \rho>\rho^*.\end{cases} \tag{3·4}$$

Equation (3·4) means that for $\rho<\rho^*$ pressure is determined by degenerate leptons. For $\rho>\rho^*$ nuclear force is taken into account by the first term of the expression of p. Units of mass, length and time are taken as

$$\left.\begin{aligned}&M=10M_\odot=2\times10^{34}\mathrm{g}\,,\\ &L=GM/c^2=1.5\times10^6\mathrm{cm}\,,\\ &T=GM/c^3=5\times10^{-5}\mathrm{sec}\,.\end{aligned}\right\} \tag{3·5}$$

Initial distribution of ε is taken as

$$\varepsilon=K\rho^{1/3}. \tag{3·6}$$

Using Eqs. (2·16), (3·4) and (3·6), we can determine the initial proper density by solving the following equation:

$$\rho=\rho_H(1-\rho_H/(\rho_H+p)\,\Omega_0{}^2\exp(-x/\lambda^2)x/\phi^4)/(1+\varepsilon)$$

iteratively. Each model is characterized by three parameters, λ, Ω_0 and K. In all the calculated models λ is 1.5. Instead of Ω_0 and K, we define more convenient parameters U, J and q as follows. The gravitational mass of the system (M_G) is determined by the asymptotic form of the conformal factor ϕ as

$$\phi=1+M_G/2/r \qquad \text{for} \quad r\to\infty\,. \tag{3·7}$$

The total baryonic mass (M_B) is defined by

$$M_B=2\pi\int_{-\infty}^{\infty}\int_0^{\infty}Q_b\cdot RdRdZ\,. \tag{3·8}$$

We define the total rotational energy ($E_{\rm rot}$) and the total internal energy ($E_{\rm int}$) by

$$E_{\rm rot}=2\pi\int_{-\infty}^{\infty}\int_0^{\infty}Q_b(\alpha u^0-1)\cdot RdRdZ \tag{3·9}$$

and

$$E_{\rm int}=2\pi\int_{-\infty}^{\infty}\int_0^{\infty}Q_b((\alpha u^0)(\varepsilon+p/\rho)-p/\rho/\alpha u^0)\cdot RdRdZ\,. \tag{3·10}$$

We define the gravitational energy ($E_{\rm grav}$) by

$$E_{\rm grav}=M_B+E_{\rm rot}+E_{\rm int}-M_G\,.$$

U and J are defined by

$$U=E_{\rm int}/E_{\rm grav} \qquad \text{and} \qquad J=E_{\rm rot}/E_{\rm grav}\,.$$

q is defined by

$$q=(\text{total angular momentum})/M_G{}^2\,.$$

ii) *Coordinate conditions*

η^A is taken to be zero. Therefore the coordinate line agrees with the normal line of $t=$constant hypersurface. As for α, the maximal slicing condition is well known, that is, α is determined by[8]

$${}^{(3)}\Delta\,\alpha=[4\pi(\rho_H+S_m{}^m)+K_{ij}K^{ij}]\alpha\equiv S_{\max}(R,Z)\alpha\,. \tag{3·11}$$

In this paper, we use a different time slice which agrees well with the maximal slicing in the case of spherically symmetric gravitational collapse.

α is determined by

$$\frac{1}{r^2}\frac{d}{dr}r^2\frac{d}{dr}\alpha = V_0 \operatorname{sech}^2(dr)\alpha\,, \tag{3·12}$$

where V_0 and d are free parameters. Namely, ${}^{(3)}\Delta$ and $S_{\max}(R, Z)$ in Eq. (3·11) are replaced by $(1/r^2)(d/dr)r^2(d/dr)$ and $V_0\operatorname{sech}^2(dr)$, respectively.

The boundary conditions of Eq. (3·12) are

$$\left.\frac{d\alpha}{dr}\right|_{r=0} = 0$$

and

$$\alpha = 1 + \text{const}/r \qquad \text{for} \quad r\to\infty\,.$$

Then the solution of Eq. (3·12) becomes

$$\alpha = [AF(\gamma, \delta, 1, u) + B(F^*(\gamma, \delta, 1, u) + F(\gamma, \delta, 1, u)\ln u)]/r\,, \tag{3·13}$$

where

$$u = e^{-2dr}/(1+e^{-2dr}), \qquad \gamma+\delta = 1\,, \qquad \gamma\delta = V_0/d^2,$$

$$F(\gamma, \delta, \varepsilon, u) = \sum_{n=1}^{\infty}\frac{\Gamma(\gamma+n)\Gamma(\delta+n)\Gamma(\varepsilon)}{\Gamma(\gamma)\Gamma(\delta)\Gamma(\varepsilon+n)}\frac{u^n}{n!}\,,$$

$$F^*(\gamma, \delta, \varepsilon, u) = \partial_\gamma F + \partial_\delta F + 2\partial_\varepsilon F\,,$$

$$A = (F^*(\gamma, \delta, 1, 1/2) - F(\gamma,\delta, 1, 1/2)\ln 2)/F(\gamma, \delta, 1, 1/2)/2/d$$

and

$$B = -1/2/d\,.$$

We want to call this slicing the hypergeometric slicing.

To determine the two parameters V_0 and d we use the maximal slicing condition (Eq. (3·11)) in this paper. V_0 and d are determined by

$$d = C/D\times\ln 2$$

and

$$V_0 = C\times d\,,$$

where

$$C = [\int_0^\infty S_{\max}(R, 0)\,dR + \int_0^\infty S_{\max}(0, Z)\,dZ]/2$$

and

$$D = [\int_0^\infty S_{\max}(R, 0)R\,dR + \int_0^\infty S_{\max}(0, Z)Z\,dZ]/2\,.$$

This is one of the methods of determining V_0 and d. As there are two free parameters which express the depth and the range of the potential for a Schrödinger type equation (Eq. (3·12)), the hypergeometric slicing will enable us to control the collapse as we like.

§ 4. Numerical results

Initial parameters of each model are shown in Table I. Since each model is characterized mainly by the value of q, we use q as a name of each model. Before showing the numerical results of each model, we discuss local conservation of angular momentum and accuracy of the numerical calculations. In Newtonian $2D$ collapse, many authors[10] have calculated the isothermal collapse under the condition that the initial density distribution is uniform and the initial angular velocity is constant. But their results are different. Some pepople say that a ring is formed. The other people say that no ring is formed. The reason for this difference is the artificial transfer of angular momentum in an Eulerian method. In Kamiya's calculation[10] no ring is formed. As he used a Lagrangian method, angular momentum is locally conserved. Norman et al.[10] carefully treated angular momentum transfer in an Eulerian method. They found that if there is little artificial transfer of angular momentum no ring is formed and the collapse is a runaway yielding central disk-like regions of increasing mass density and flatness. The above experience in Newtonian $2D$ collapse tells us that we must carefully treat the angular momentum conservation in the general relativistic $2D$ code, too. We define $M(l)$ as the mass of a star with specific angular momentum

Table I. Initial conditions and main results of all the calculated models. M_B, M_G, U, J and q are total baryon mass, gravitational mass, the ratio of total internal energy to gravitational energy, the ratio of total rotational energy to gravitational energy and total angular momentum divided by M_G^2, respectively. Units are shown in the text.

Name of Model	M32	M48	M56	M64	M80	M86	M95	M109	M137
M_B	0.977	0.969	0.963	0.957	0.941	0.931	0.921	0.897	0.833
M_G	0.882	0.884	0.886	0.886	0.890	0.892	0.894	0.899	0.911
U	0.20	0.20	0.20	0.20	0.21	0.21	0.22	0.23	0.25
J	0.05	0.12	0.17	0.22	0.36	0.45	0.55	0.79	1.56
q	0.32	0.48	0.56	0.64	0.80	0.86	0.95	1.09	1.37
Apparent Horizon?	YES	YES	YES	YES	YES	YES	NO	NO	NO
Ring of Q_b?	NO	NO	NO	NO	NO	YES	YES	YES	YES
Its Location ($R=$)	—	—	—	—	—	3.3 (weak)	3.3	3.3	4.6
Ring of ρ?	NO	YES	YES	YES	YES	YES	YES	YES	YES
Its Location ($R=$)	—	0.8 (weak)	1.2 (weak)	2.4	2.4	2.8	2.8	3.3	3.9
Minimum of $\sqrt{H}$ ($R=$)	0.8 (weak)	1.4	2.0	2.4	2.4	2.8	2.8	2.8	3.3

less than or equal to l,

$$M(l)=2\pi\sum_{l'\leq l}Q'_b R'\,\Delta R'\cdot\Delta Z', \tag{4·1}$$

where

$$l'=\Omega' R'^2. \tag{4·2}$$

From Eqs. (2·13), (2·14) and (2·17), we can see easily $M(l)$ should be time independent if the angular momentum is conserved locally. $M(l)$ is shown for M64 in Fig. 1. Open circles show $M(l)$ at $t=0$ and lozenges show $M(l)$ at $t=12.4$ when an apparent horizon*) is already formed. We can see the local conservation of angular momentum is quite well.

In Ref. 8) accuracy of a constraint equation (A.C.Eq.) is defined by

$$\text{A.C.Eq.}=\left|1-\frac{\text{R.H.S. of the constraint equation}}{\text{L.H.S. of the constraint equation}}\right|. \tag{4·3}$$

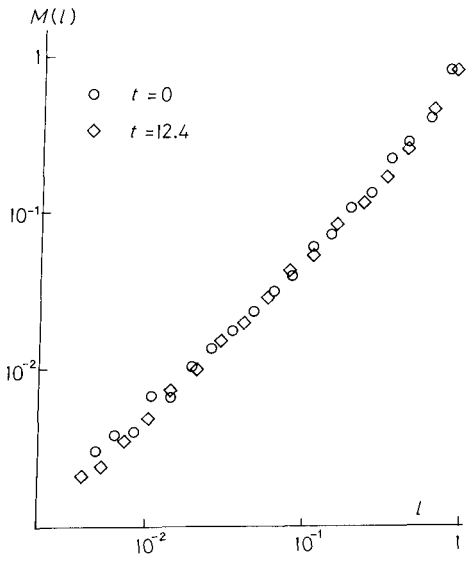

Fig. 1. The specific angular momentum spectrum for M64. The quantity $M(l)$ is the total mass in the star with specific angular momentum less than or equal to $l=R^2\Omega$. Open circles are $M(l)$ at $t=0$. Lozenges are $M(l)$ at $t=12.4$ when an apparent horizon is already formed.

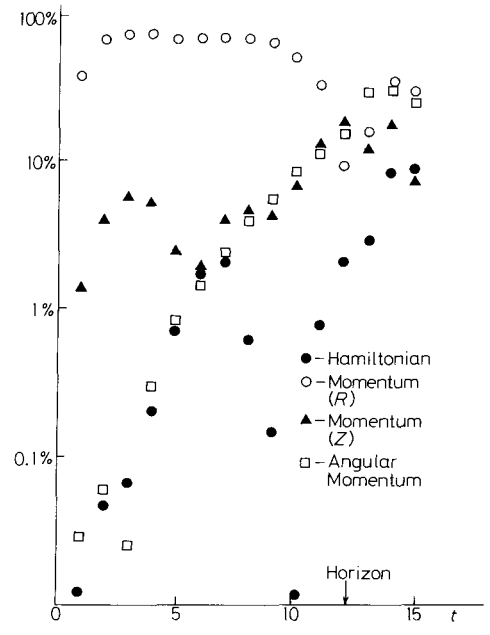

Fig. 2. Accuracy of constraint equations (A. C. Eq.) at the center for M64. An arrow shows the time when an apparent horizon is formed. We can see A. C. Eq.'s are 20% or so at that time.

*) A method of determining an apparent horizon is the same as that in Ref. 11).

A.C.Eq. should be zero if we can solve the basic equations exactly. In numerical calculation, A.C.Eq. tells us the effect of the truncation error and the viscosity terms to the true solution quantitatively. A.C.Eq.'s for M64 are shown in Fig. 2. For simplicity the time variation of A.C.Eq.'s at the center is shown. We can see the accuracy of momentum constraint equations (Eq. (2·6)) is worse than that of the Hamiltonian (Eq. (2·5)) and the angular momentum constraint equations (Eq. (2·9)). As χ_{AB} is determined by the second and the first derivative of the metric tensor, the accuracy of the momentum constraint equations is essentially that of the third derivative of the metric tensors. On the other hand the accuracy of the Hamiltonian constraint equation is essentially that of the second derivative of the metric tensors and the accuracy of the angular momentum constraint equation is essentially that of the first derivative of E^A. Figure 2 shows A. C. Eq.'s are 20% or so at the time when an apparent horizon is formed. Therefore it can be said that the accuracy of our numerical calculation is good enough.

The numerical results are summarized as follows. For slowly rotating models, for example M32, the distribution of ρ and Q_b becomes oblate shape as the collapse proceeds. An apparent horizon is formed and matter is swallowed into the black hole completely. In this case the effect of rotation is only to deform the matter distribution. For rather rapidly rotating models, for example M80, the shape of Q_b is disk-like (Fig. 3 (a)) but there appears a ring-like peak of ρ which is inside the apparent horizon (Fig. 3 (b)). At this peak $E_A E^A$ is very large (Fig. 3 (b)) and $\sqrt{H}$ takes a minimum value (Table I). The reason for this behavior can be interpreted as the general relativistic effect of rotation. Taking a trace of Eq. (2·2), we have

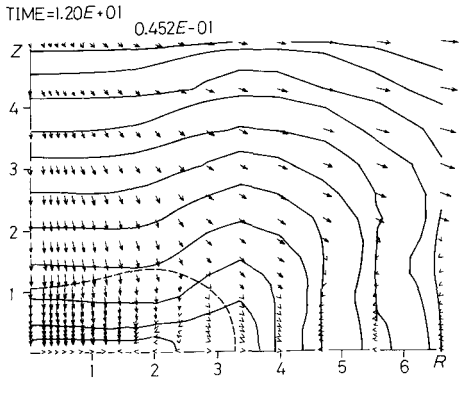

Fig. 3. (a) Contour lines of Q_b for M80 at $t=12.0$. Each line corresponds to $Q_b=(Q_b)_{max}\cdot 10^{-n/2}$ where $(Q_b)_{max}=4.52\cdot 10^{-2}$ for $n=1, 2, \cdots, 11$. Arrows show vectors (J_A/Q_b). The apparent horizon is shown by the dashed line.

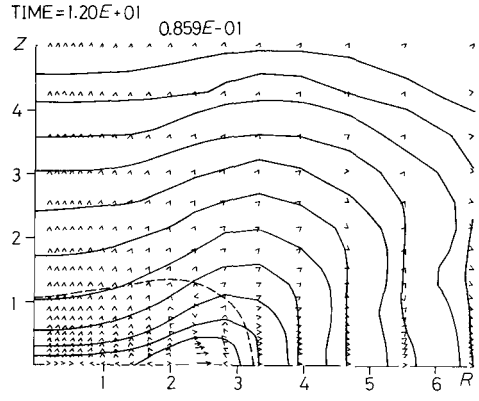

(b) Contour lines of proper density (ρ) for M80 at $t=12.0$. Each line corresponds to $\rho=\rho_{max}\cdot 10^{-n/2}$ where $\rho_{max}=8.59\cdot 10^{-2}$ for $n=1, 2, \cdots, 11$. The apparent horizon is shown by the dashed line. Arrows show vectors E^A.

$$\partial_0\chi=\frac{1}{2}\alpha E_A E^A+\text{other terms}\,. \tag{4·4}$$

Multiplying H^{AB} both sides of Eq. (2·1), we obtain for $\eta^A=0$

$$\partial_0(\ln\sqrt{H})=-\alpha\chi\,. \tag{4·5}$$

We write Eq. (2·9) again

$$\partial_A(\lambda^2\sqrt{H}E^A)=16\pi Q_b R^3\Omega\,. \tag{4·6}$$

We already knew that the angular momentum density behaves like "charge density" for E^A. The distribution of Q_b is disk-like (Fig. 3 (a)). So the distribution of "charge density" becomes ring-like as J_ϕ is zero at $R=0$ and $R=\infty$. This "charge density" makes a ring-like peak of E^AE_A (see Eq. (4·6)). From Eq. (4·4), we can see α increases with the increase of E^AE_A. The increase of χ means the decrease of $\sqrt{H}$ (see Eq. (4·5)). Finally the decrease of $\sqrt{H}$ makes E^AE_A large. Therefore this cycle makes E^AE_A and χ larger and $\sqrt{H}$ smaller. A ring-like minimum of $\sqrt{H}$ makes a ring-like peak of ρ although Q_b is disk-like. This ring will develop to a ring-like singularity but the numerical calculation is stopped by the Courant condition. For rapidly rotating models, for example, M95, no apparent horizon is formed. (See Table I.) Q_b shows a central disk plus a slowly expanding ring. (Fig. 4(a).) ρ shows a ring-like peak with the maximum of E^AE_A. (Fig. 4 (b).) In this case this ring-like peak may develop to a naked singularity by the same mechanism as in rather rapidly rotating models. For very rapidly rotating models, for example M137, Q_b shows a central disk plus a fast expanding ring. (Fig. 5(a).) ρ shows a weak ring-like peak but E^AE_A shows a ring-like

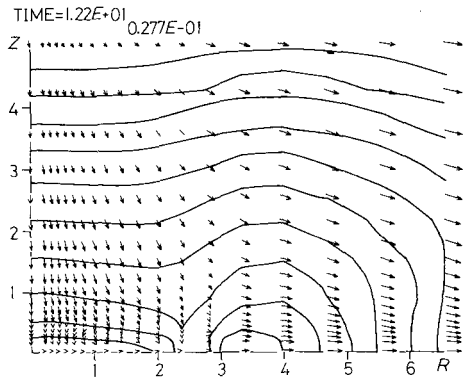

Fig. 4. (a) Contour lines of Q_b for M95 at $t=12.2$. Each line corresponds to $Q_b=(Q_b)_{\max}\cdot10^{-n/2}$ where $(Q_b)_{\max}=2.77\cdot10^{-2}$ for $n=1, 2, \cdots, 10$. Arrows show vectors (J_A/Q_b).

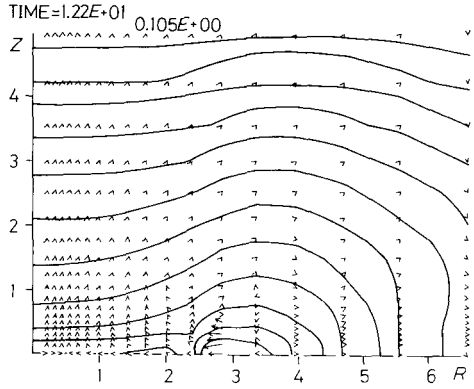

(b) Contour lines of proper density (ρ) for M95 at $t=12.2$. Each line corresponds to $\rho=\rho_{\max}\cdot10^{-n/2}$ where $\rho_{\max}=1.05\cdot10^{-1}$ for $n=1, 2, \cdots, 12$. Arrows show vectors E^A.

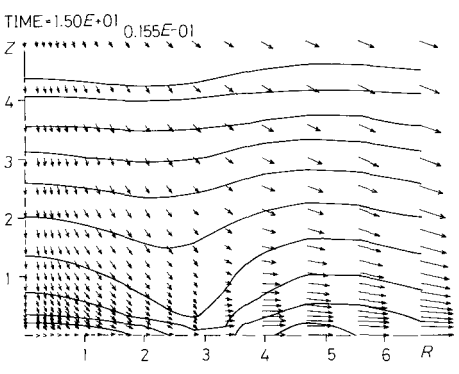

Fig. 5. (a) Contour lines of Q_b for M137 at $t=15.0$. Each line corresponds to $Q_b=(Q_b)_{\max}\cdot 10^{-n/2}$ where $(Q_b)_{\max}=1.55\cdot 10^{-2}$ for $n=1, 2, \cdots, 10$. Arrows show vectors (J_A/Q_b).

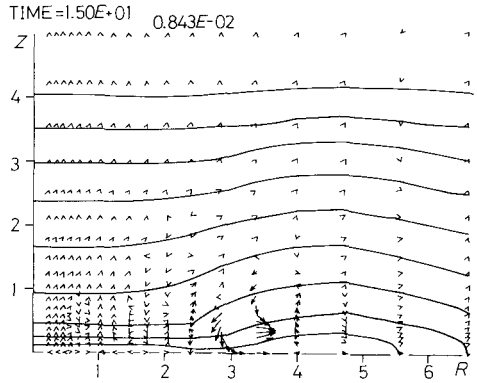

(b) Contour lines of proper density (ρ) for M137 at $t=15.0$. Each line corresponds to $\rho=\rho_{\max}\cdot 10^{-n/2}$ where $\rho_{\max}=8.43\cdot 10^{-3}$ for $n=1, 2, \cdots, 9$. Arrows show vectors E^A.

peak. In this case the numerical calculation does not proceed further as α becomes very small even in the ring region.

§ 5. Discussion and concluding remarks

As far as the numerical calculations in this paper are concerned, an important conclusion is that if q is larger than about unity an apparent horizon is not formed. The Kerr black hole with $q=1$ corresponds to the maximum Kerr solution. Coincidence of this number with 0.95 in the numerical calculation is surprising. It can be said at least that the numerically generated rotating black holes for $q\lesssim 0.95$ in this paper look like the Kerr black holes in a sense that they have apparent horizons and no naked singularities although it is very difficult to prove that they are exactly the Kerr black holes. For some models with $q\gtrsim 0.95$, it is suggested that a naked singularity may appear.

As we saw in § 4, E^A plays an important role in the general relativistic collapse of a rotating star. The interpretation of the effects of E^A to the collapse given in § 4 is only the beginning of the true understanding of these electromagnetic like fields in the $[(2+1)+1]$-formalism of the Einstein equations. It is expected that if we use a different initial distribution of angular momentum from Eq. (3·1) the structure of black holes will be different from Fig. 3. For example, if "charge density" (J_ϕ) has two or three peaks, ρ may have two or three ring-like peaks.

Next we will mention the choice of the time slicing. We have recalculated M48 with the maximal slicing condition. In this case, an apparent horizon is not formed. The reason is that the proper time of the co-moving observer stops

increasing too soon. Therefore the maximal slicing is not good to know the structure of rotating black holes. However the hypergeometric slicing is not the best one, either. In M80, α is about 0.5 or so at the ring of ρ. Therefore not α but the Courant condition stops the numerical calculation. For M137, α becomes too small even at the ring because the expansion velocity is too large. (See Eq. (3·13).) Better time slicing which stops the proper time of the normal line observer at the ring position is needed to know the structure of singularities of rotating black holes and naked singularities which may appear for $q \gtrsim 0.95$.

Acknowledgements

The author would like to thank Professor C. Hayashi and Professor H. Sato for continuous encouragement and critical discussions. He wishes to thank Dr. K. Maeda, Messrs. S. Miyama, M. Sasaki, H. Kodama and K. Oohara for useful comments and discussions. This work was partly carried out under the collaborating research program at the Institute of Plasma Physics, Nagoya University. He is indebted to Soryushi Shogakukai for the financial aid.

Appendix

In this appendix, we derive Eqs. (2·1) to (2·9). If we apply Geroch's formalism[12] to an axially symmetric system, we obtain

$$ {}^{(3)}R_{\mu\nu} = (2\lambda^4)^{-1}[\omega_\mu\omega_\nu - h_{\mu\nu}\omega^\rho\omega_\rho] + \lambda^{-1}D_\mu D_\nu\lambda + 8\pi\left(\mathcal{T}_{\mu\nu} - \frac{1}{2}h_{\mu\nu}(\mathcal{T}_\rho{}^\rho + \lambda^{-2}\mathcal{T})\right), \tag{A·1} $$

$$ \lambda^{-1}D^\rho D_\rho\lambda = -(2\lambda^4)^{-1}\omega^\rho\omega_\rho - 4\pi(\lambda^{-2}\mathcal{T} - \mathcal{T}_\alpha{}^\alpha), \tag{A·2} $$

$$ D_{[\mu}\omega_{\nu]} = 8\pi\lambda\varepsilon_{\mu\nu\rho}\mathcal{T}^\rho, \tag{A·3} $$

$$ D^\rho[\lambda^{-3}\omega_\rho] = 0, \tag{A·4} $$

where

$$ \lambda^2 = \xi_\mu\xi^\mu, \tag{A·5} $$

$$ h_{\mu\nu} = g_{\mu\nu} - \lambda^{-2}\xi_\mu\xi_\nu, \tag{A·6} $$

$$ \omega_\mu = \varepsilon_{\mu\nu\rho\sigma}\xi^\nu\nabla^\rho\xi^\sigma, \tag{A·7} $$

$$ \varepsilon_{\mu\nu\rho} = \lambda^{-1}\xi^\sigma\varepsilon_{\mu\nu\rho\sigma}, \tag{A·8} $$

and ξ^μ, ∇^μ, D^μ and ${}^{(3)}R_{\mu\nu}$ reperesent a rotational Killing vector, four-dimensional covariant differentiation, three-dimensional covariant differentiation and three-

dimensional Ricci tensor, respectively. $\mathcal{T}$, $\mathcal{T}_\mu$ and $\mathcal{T}_{\mu\nu}$ are defined by

$$\mathcal{T} = T_{\mu\nu}\xi^\mu\xi^\nu,$$

$$\mathcal{T}^\rho = h^{\rho\mu}\xi^\nu T_{\mu\nu}$$

and

$$\mathcal{T}_{\rho\sigma} = h_\rho{}^\mu h_\sigma{}^\nu T_{\mu\nu},$$

where $T_{\mu\nu}$ is energy-momentum tensor of matter. Next we define a projection tensor*) as

$$H_{ab} = h_{ab} + n_a n_b, \tag{A·9}$$

where n_a is a unit normal vector of t=constant hypersurface. We define α (lapse function) and η^A (shift vector) as

$$ds^2 = h_{ab}dx^a dx^b = -\alpha^2 dt^2 + H_{AB}(dx^A + \eta^A dt)(dx^B + \eta^B dt).$$

χ_{AB} appeared in Eq. (2·1) is the extrinsic curvature with respect to H_{AB}. Furthermore we define various quantities appeared in Eqs. (2·1) to (2·9) as

$$\chi = \chi_A{}^A, \qquad \lambda K_\phi{}^\psi = -n^\mu \partial_\mu \lambda,$$

$$E^A = \varepsilon^{AB} H_B{}^b \omega_b \lambda^{-2}, \qquad B_\phi = n_a \omega^a \lambda^{-2},$$

$$\varepsilon_{AB} = n^c \varepsilon_{CAB}, \qquad \rho_H = n_a n_b \cdot \mathcal{T}^{ab},$$

$$J_\phi = -n_a \mathcal{T}^a, \qquad H = \det(H_{AB}),$$

$$J^A = -n_a H_b{}^A \mathcal{T}^{ab}, \qquad S^A = H_b{}^A \mathcal{T}^b$$

and

$$S_{AB} = H_{Aa} H_{Bb} \mathcal{T}^{ab}.$$

If we carry out projection of all the tensors appeared in Eqs. (A·1) to (A·8), we obtain Eqs. (2·1) to (2·9).

References

1) W. Israel, Phys. Rev. **164** (1967), 1776.
2) B. Carter, Phys. Rev. Letters **26** (1971), 331.
3) D. C. Robinson, Phys. Rev. Letters **34** (1975), 905.
4) For example,
A. Tomimatsu and H. Sato, Prog. Theor. Phys. **50** (1973), 95.
W. Kinnersley and D. M. Chitre, J. Math. Phys. **19** (1978), 2037.
C. Hoenselaers, W. Kinnersley and B. C. Xanthopoulos, Phys. Rev. Letters **42** (1979), 481.
D. Kramer and G. Neugebauer, Phys. Letters **75A** (1980), 259.
M. Yamazaki, Prog. Theor. Phys. **64** (1980), 861.
5) P. Yodzis, H. J. Seifert and Müller zum Hagen, Comm. Math. Phys. **34** (1973), 135.

*) Small Latin indices refer to the range 0, 1, 2 and capital Latin indices to the range 1, 2.

6) T. Nakamura, K. Maeda, S. Miyama and M. Sasaki, *Proceedings of the Second Marcel Grossmann Meeting on General Relativity* (North Holland, Amsterdam, 1980).
7) K. Maeda, M. Sasaki, T. Nakamura and S. Miyama, Prog. Theor. Phys. **63** (1980), 719.
8) T. Nakamura, K. Maeda, S. Miyama and M. Sasaki, Prog. Theor. Phys. **63** (1980), 1229.
9) J. R. Wilson, *Sources of Gravitational Radiation*, ed. by L. Smarr (Cambridge University Press, Cambridge, 1979), p. 423.
10) R. B. Larson, Month. Notices. Roy. Astron. Soc. **156** (1972), 437.
W. Tscharnuter, Astron. and Astrophys. **39** (1975), 207.
D. C. Black and P. Bodenheimer, Astrophys. J. **206** (1976), 138.
K. Nakazawa, C. Hayashi and M. Takahara, Prog. Theor. Phys. **56** (1976), 515.
Y. Kamiya, Prog. Theor. Phys. **58** (1977), 802.
M. L. Norman, J. R. Wilson and R. T. Barton, Astrophys. J. **239** (1980), 968.
P. Bodenheimer and W. Tscharnuter, Astron. and Astrophys. **74** (1979), 288.
11) M. Sasaki, K. Maeda, S. Miyama and T. Nakamura, Prog. Theor, Phys. **63** (1980), 1051.
12) R. Geroch, J. Math. Phys. **12** (1971), 918.